

# Tear and wear of thermoplastic elastomers from blends of poly(propylene) and ethylene vinyl acetate rubber

SABU THOMAS, B. R. GUPTA, S. K. DE

*Rubber Technology Centre, Indian Institute of Technology, Kharagpur 721 302, India*

Tear and wear properties of thermoplastic elastomers from blends of poly(propylene) (PP) and ethylene vinyl acetate rubber have been studied with special reference to the effect of blend ratios and dynamic crosslinking of the rubber phase. Both tear and wear resistance of the composites were found to increase with increasing proportion of the PP phase. Dynamic crosslinking of the blends containing higher proportions of the rubber phase (>60%) increases the wear and tear properties, but blends containing higher proportions of the plastic phase show a decrease in properties due to the degradation of the PP phase. Attempts have been made to correlate the changes in properties with the morphology of system. In order to understand the mechanism of failure, the tear and wear fracture surfaces have been examined by scanning electron microscopy. The fractographs have been correlated with the strength and type of failure of these blends.

## 1. Introduction

The blending of a thermoplastic and an elastomer gives a class of rubbery materials known as thermoplastic elastomers. These materials possess the very good physical properties of elastomers and the excellent processing characteristics of thermoplastics, thereby bridging the gap between the conventional elastomers and thermoplastics. Among the various types of thermoplastic elastomers, those prepared by melt-mixing of a crystalline thermoplastic material and an elastomer under high shearing action have gained considerable attention due to the simple method of preparation and easy attainment of the desired physical properties by varying the blend ratios [1–5]. It has been shown that the addition of small quantities of crosslinking agent during the mixing operation improves the final properties of high rubber blends. This type of crosslinking is known as dynamic crosslinking [6, 7]. Several studies have been reported on the properties and applications of various thermoplastic–elastomer blends [8–12]. The major area of application of this type of material is in footwear, where processes such as abrasion, flexing and tear are the prominent factors leading to the failure of the products. Abrasion of polymeric materials has been studied by many authors [13–19]. Schallamach [13, 14] was the first to study in detail the abrasion pattern of rubber surfaces. Klitenik and Ratner [15], Reznikovskii and Brodskii [16] and Lancaster [17] have done extensive work on the mechanism of abrasion. The mechanism of tear fracture of rubber vulcanizates has been studied in detail [20, 21]. The role of rubber particles in the mechanism of tear propagation in rubber-modified thermoplastics and thermosets has also been reported [22–25]. Scanning electron microscopy (SEM) has been found to be a valuable tool in

studying the fracture mechanism of rubber vulcanizates and rubber-based composites [26–34]. In this paper we have studied the effect of blend ratios and the influence of dynamic crosslinking of the elastomer phase on the tear and wear of thermoplastic poly(propylene) (PP) and ethylene vinyl acetate (EVA) rubber blends.

## 2. Experimental procedure

### 2.1. Materials used

Ethylene vinyl acetate used in the present study contains 45% (wt %) vinyl acetate. The material was supplied by Bayer AG (W. Germany). Poly(propylene) used for this study was isotactic poly(propylene) (grade Koylene M0030) supplied by Indian Petrochemicals Corp., Baroda, India. The characteristics of the above materials are given in Table I.

### 2.2. Preparation of the blends and test samples

Formulations of the blends are given in Table II. The blend ratios are denoted by  $E_0$ ,  $E_{30}$ ,  $E_{40}$ ,  $E_{50}$ ,  $E_{60}$ ,  $E_{70}$  and  $E_{100}$  where the subscripts denote the weight percentage of EVA in the blend. Dynamically crosslinked blends are denoted by a superscript “d”. For example the notation  $E_{70}^d$  indicates a 70:30 EVA:PP blend containing dicumyl peroxide (DCP) crosslinking agent. Blends of EVA and PP were prepared in a Brabender Plasticorder model PLE 330 (Brabender OHG, West Germany), using a cam-type mixer with a rotor speed of 80 r.p.m. and the mixer chamber temperature set at 180°C. The total mixing time was fixed to 7 min. In preparing the blends, PP was melted first in the mixer and then EVA was added. The blend was allowed to mix for 2 min. At the end of the second minute, curatives were added and the mixing was

TABLE I Characterization data for the base materials used

Property	Material	
	PP	EVA
Density ( $\text{g cm}^{-3}$ )	0.91	0.975
Number-average molecular weight, $\bar{M}_n$	106 000	–
Mooney viscosity ML(4) 100°C	–	30
Weight-average molecular weight	530 000	–
Intrinsic viscosity (benzene, 30°C) ( $\text{dl g}^{-1}$ )	4.45	–

continued for 4 min. The blend was taken out and sheeted through a laboratory mill at 2.00 mm nip setting. The sheeted material was cut into small pieces and again mixed in the plasticorder at 180°C for one minute and then finally sheeted out in the mill so as to obtain relatively uniform dispersion of the ingredients. The sheeted-out stock was compression-moulded at 200°C for three minutes in specially designed moulds so that the mould with the sample inside could be cooled immediately after moulding while keeping the same under compression. Samples for tear tests were punched from the moulded sheets and were of size 15 cm  $\times$  15 cm  $\times$  0.2 cm. Abrasion test pieces (2  $\times$  2  $\times$  1 cm) were moulded directly.

### 2.3. Physical testing

The tear strength of the samples was determined at  $25 \pm 2^\circ\text{C}$  according to the ASTM D624-81 test method using 90° angle test pieces. The measurement was carried out in an Instron Universal Testing Machine (Model 1195) at a crosshead speed of 500 mm min<sup>-1</sup>.

The abrasion resistance of the samples was tested in a Dupont Abrader (Dupont, USA) using a silicon carbide abrasive paper of grit size 320. The abrasion process was unidirectional. The speed of rotation of the abrasive disc was 40 r.p.m. and the normal load was 3.26 kg. The radius of the wheel was 0.082 m. The samples were abraded for 20 min after an initial abrasion period of 5 min. The initial abrasion was necessary to obtain a uniform surface. The volume loss was expressed in cubic metres (m<sup>3</sup>).

### 2.4. Scanning electron microscopy studies

The SEM observations of the tear and wear failure surfaces were made using a Philips Model 500 scanning electron microscope. The failure surface of the test samples was carefully cut out from one of the test pieces without touching the surfaces and then sputter-

coated with gold within 24 h of testing. The specimens were stored in a desiccator before and after gold coating until the SEM observations were made, in order to avoid contamination. In taking photographs, the tilt was kept at 0° in all cases. Fig. 1 shows the details of the test specimen, failure surface and scan area of the tear and abrasion test samples.

## 3. Results and discussion

Our earlier studies [35] on the morphology of EVA–PP blends showed a two-phase structure in which the EVA phase was dispersed as domains in the continuous PP matrix at lower proportions ( $\leq 50\%$ ) of the rubber phase, but when the rubber phase is more ( $\geq 60\%$ ), this phase also formed a continuous phase. The 70:30 EVA:PP acts as a interpenetrating two-phase system. The mechanical properties such as tensile strength, modulus, elongation at break, impact strength and flexural modulus depend on the morphology of the system.

### 3.1. Tear properties

The tear strength values of the blends as a function of the weight percent of EVA are given in Fig. 2. For both crosslinked and uncrosslinked systems, the tear strength values decrease with increasing proportion of the rubber phase. This is due to the decrease in crystallinity of the system with the increase of rubber content. The strength of EVA–PP blends depends on the strength of the PP matrix, which in turn depends on the extent of crystallinity. Martuscelli and co-workers [36, 37] have shown that the spherulite growth of isotactic poly(propylene) in blends with rubber is hindered by the presence of the rubber phase. Hence the observed drop in tear strength of the blends with increase in rubber content is due to the reduction in crystallinity. As compared to uncrosslinked systems, dynamically crosslinked samples of high plastic blends ( $\geq 50\%$ ) show lower values of tear strength. This is associated with the degradative action of DCP on the PP phase [6, 12, 35]. Our earlier studies [35] have shown that DCP has two major effects on the blends, degradation of the PP phase and crosslinking of the EVA phase. The degradation of PP is predominant at higher proportion ( $\geq 50\%$ ) of PP, while crosslinking of EVA is prominent at higher proportions of EVA phase. When the rubber phase is more and continuous in nature, dynamic crosslinking increases the tear strength.

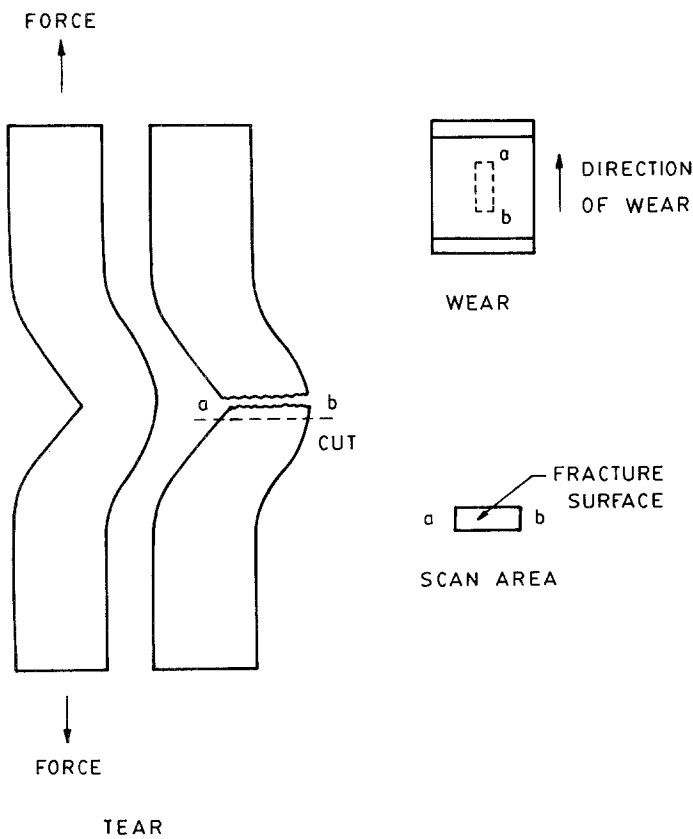
TABLE II Compositions of the blends

Components	Mix No.											
	E <sub>0</sub>	E <sub>30</sub>	E <sub>40</sub>	E <sub>50</sub>	E <sub>60</sub>	E <sub>70</sub>	E <sub>100</sub>	E <sub>30</sub> <sup>d</sup>	E <sub>40</sub> <sup>d</sup>	E <sub>50</sub> <sup>d</sup>	E <sub>60</sub> <sup>d</sup>	E <sub>70</sub> <sup>d</sup>
EVA	0	30	40	50	60	70	100	30	40	50	60	70
PP	100	70	60	50	40	30	0	70	60	50	40	30
DCP*	–	–	–	–	–	–	–	0.6	0.6	0.6	0.6	0.6
TAC <sup>†</sup>	–	–	–	–	–	–	–	0.7	0.7	0.7	0.7	0.7
MgO <sup>†</sup>	–	–	–	–	–	–	–	0.7	0.7	0.7	0.7	0.7

\*Dicumyl peroxide (DCP) crosslinking agent was supplied by Bengal Waterproof Works Ltd, Calcutta. The DCP dosage was based on the rubber phase alone.

<sup>†</sup>Triallyl cyanurate (TAC) and magnesium oxide (MgO) act as coagents for DCP curing. The dosage was based on the rubber phase alone. The materials were supplied by Bengal Waterproof Works Ltd, Calcutta.

Figure 1 Samples for tear and wear tests showing fracture surface and scan area.



The tear curves of the uncrosslinked and cross-linked samples are given in Figs 3 and 4, respectively. The nature of the failure can be understood from the tear curves. In the case of PP (Fig. 3) the load reaches a maximum and then abruptly drops to zero. This indicates brittle-type failure. As the proportion of the rubber increases, the ductile nature and yielding tendency increase (Fig. 3). In the case of  $E_{70}$  and  $E_{100}$ , the samples elongate to a large extent to reach the failure point. The tear curves of dynamically cross-linked samples (Fig. 4) show some variation from that of the uncrosslinked samples. The tear curve of  $E_{30}^d$  is

of brittle type similar to that of PP. This is due to the fact that the degradation of the PP phase make the sample more brittle. In the case of other samples ( $E_{40}^d$ ,  $E_{50}^d$ ,  $E_{60}^d$  and  $E_{70}^d$ ) the deformation is of elastic type. Unlike uncrosslinked blends, the ductile nature and yielding behaviour are completely absent. As compared to the uncrosslinked samples, in this case the elongation of the samples during tearing is also reduced considerably.

### 3.1.1. Tear fractographs

In tear, the nucleation of failure and microfracture

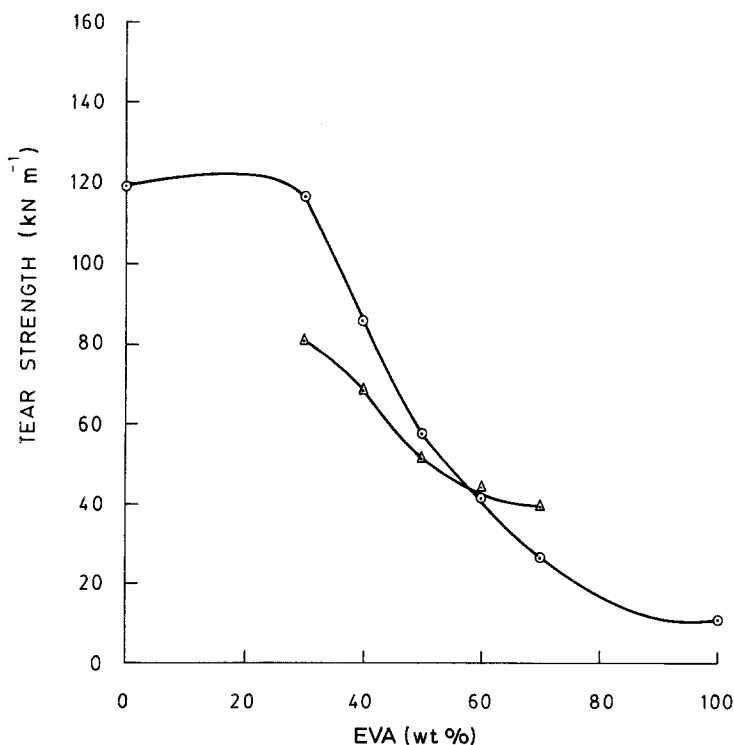


Figure 2 Effect of weight percentage of EVA on tear strength: (○) uncrosslinked, (Δ) dynamically cross-linked.

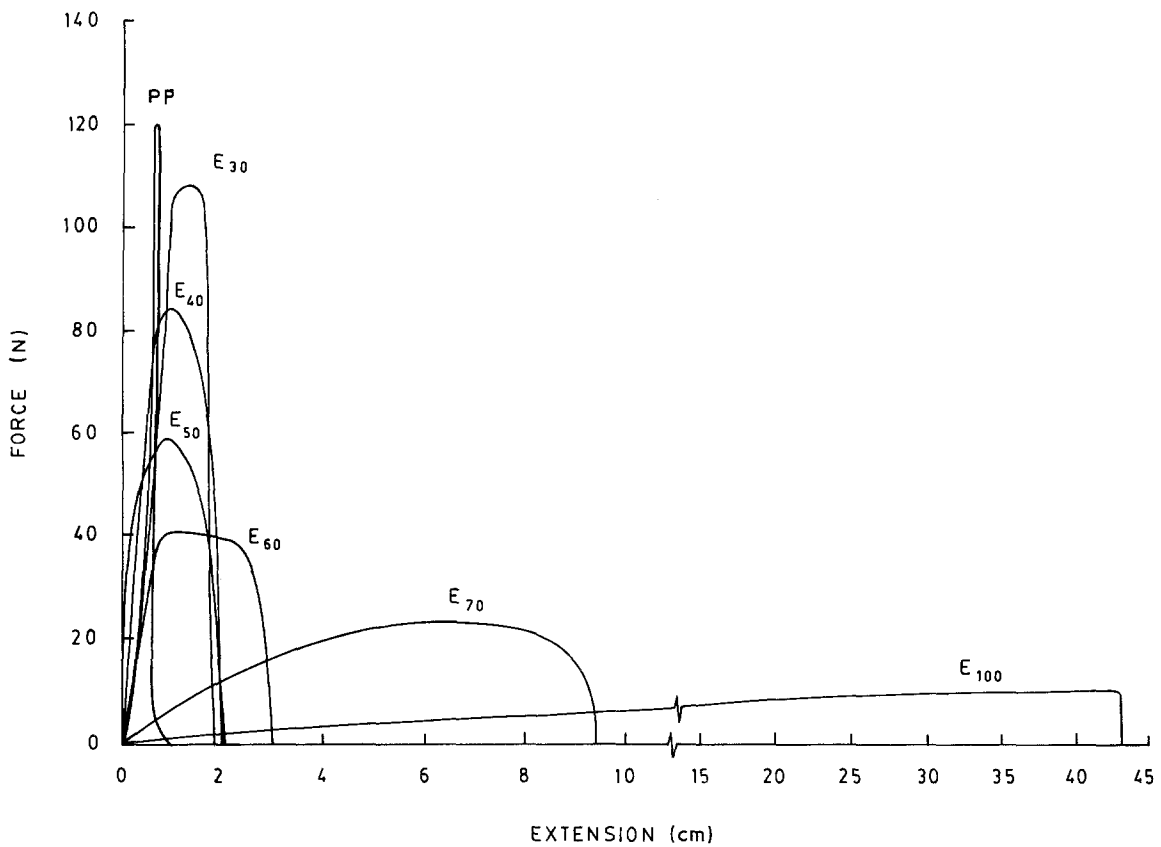


Figure 3 Tear curves of the uncrosslinked samples.

occur almost in the region of high stresses, at the tip of the tear. Hence the dissipation of stresses near the tip of the crack determines the resistance to tearing. The nature of failure and the process of stress dissipation can be understood by a careful examination of the tear failure surfaces.

Fig. 5 shows the tear failure surface of PP. The presence of many parallel fracture paths in different planes indicates the brittle nature of the failure. The addition of rubber makes the material ductile. This is evident from the fracture surface of  $E_{30}$  (Fig. 6). It shows vertical tear paths. The fibrils on the failure surface along the direction of propagation of the crack indicate the ductile nature of the failure. Engel *et al.* [38] suggested that fibril formation is a characteristic of ductile-type failure. The dynamically crosslinked sample ( $E_{30}^d$ ) shows brittle-type fracture as evident

from the discontinuous tear paths in different planes (Fig. 7). The load-extension curves (Fig. 4) also support the above views.

The failure surface of  $E_{50}$  (Fig. 8) shows ductile failure with a high extent of plastic deformation, as evidenced by the presence of fibrillar structure and peaks. The presence of voids in the surface is associated with the detachment of the dispersed rubber phase from the plastic matrix. The corresponding crosslinked sample ( $E_{50}^d$ ) shows elastic-type deformation with irregular tear paths (Fig. 9). The lack of fibrils and peaks indicate elastic type failure. Further increase in the proportion of the rubber in the blend make the rubber phase continuous. This is evident from the fracture surface of  $E_{70}$  which shows ductile-type failure with an elongated continuous dimple structure (Fig. 10). The dynamically crosslinked sample ( $E_{70}^d$ ) shows elastic-type deformation with continuous tear paths (Fig. 11). The absence of

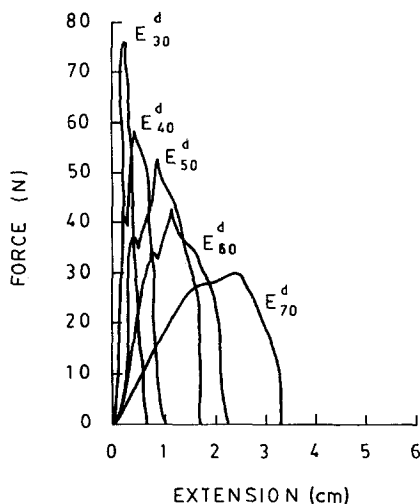


Figure 4 Tear curves of dynamically crosslinked samples.

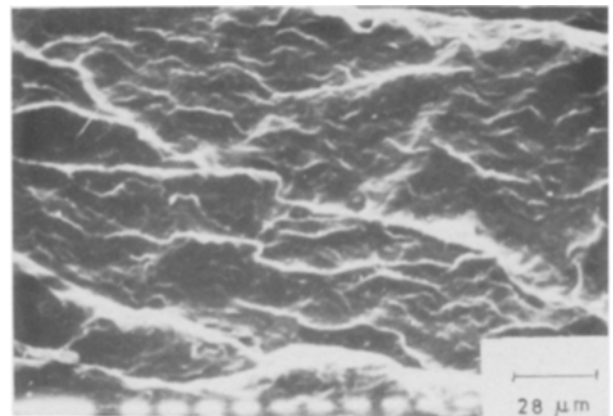


Figure 5 Tear failure surface of PP showing brittle fracture.

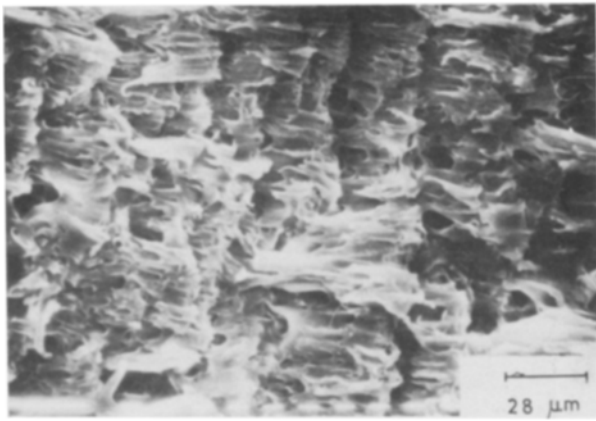


Figure 6 Tear failure surface of E<sub>30</sub> showing vertical fracture paths and fibrils.

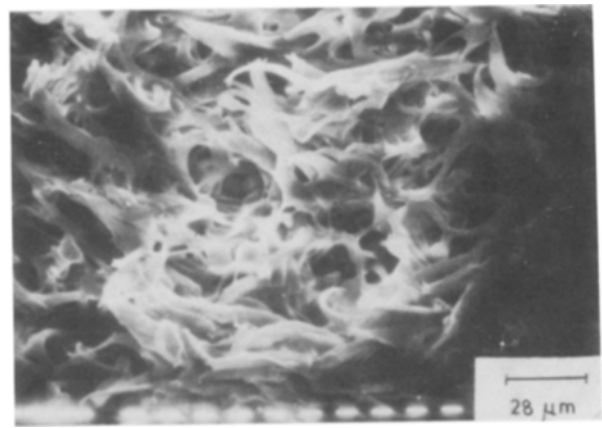


Figure 8 Tear failure surface of E<sub>50</sub> showing ductile fracture.

fibrils and dimples confirms the elastic nature of the failure.

### 3.2. Wear properties

The abrasion of elastomers involves complex processes such as microcutting and tearing, crack growth, fatigue and thermal and oxidative degradation [39]. Depending on the type of polymer and the conditions of abrasion, any one of the above factors may play a prominent role in the failure of the sample by abrasion. Hence, the abrasion resistance is related to the strength of the matrix, resistance to thermo-oxidative degradation, crack growth resistance under dynamic conditions, frictional force and the nature of the abrasive. Reznikovskii and Brodskii [16] have described the different types of wear associated with the abrasion of polymers. These include fatigue wear, abrasive wear and wear by roll formation. The basis of fatigue wear is failure of the surface layer of rubber as a result of manifold deformations. Fatigue wear does not cause any visible scratches on the worn surface. Unidirectional abrasive wear is characterized by longitudinal furrows on the surface. The frictional wear of elastomers is characterized by vertical ridge formation and subsequent removal of the ridges in the course of abrasion. Thus the patterns appearing on the abraded surfaces are indicative of the type of wear and are helpful in understanding the mechanism of wear.

Fig. 12 shows the abrasion loss of the samples with increasing proportions of EVA. The abrasion loss of

pure EVA could not be established, as the material chipped out during the first minute of the abrasion due to its very poor abrasion resistance. In the case of the uncrosslinked samples, the abrasion loss increases with increasing proportion of EVA phase and the increase of volume loss is much larger at higher proportions of EVA phase. The dynamically crosslinked samples show a steady increase in volume loss with increasing proportion of EVA. At lower proportions of the EVA phase ( $\leq 50\%$ ) the dynamically crosslinked samples show more abrasion loss as compared to the uncrosslinked samples. But at higher proportions of the rubber phase, dynamic crosslinking decreases the volume loss. This behaviour can be correlated with the mechanical properties and morphology of the system. Previous studies [19, 40] also show that wear properties are dependent on the mechanical strength and morphology of the system. The mechanical properties of the blends are given in Table III. It can be seen that on increasing the proportion of the EVA phase, the mechanical properties such as tensile strength, tear strength, hardness, modulus and flexural modulus decrease. The dynamically crosslinked samples show lower mechanical strength as compared to the uncrosslinked samples at higher proportions of the PP phase, due to the predominant degradation of PP as explained earlier. But when the rubber phase is 70%, the mechanical properties are marginally improved due to crosslinking of the EVA phase which overshadows the degradation. The

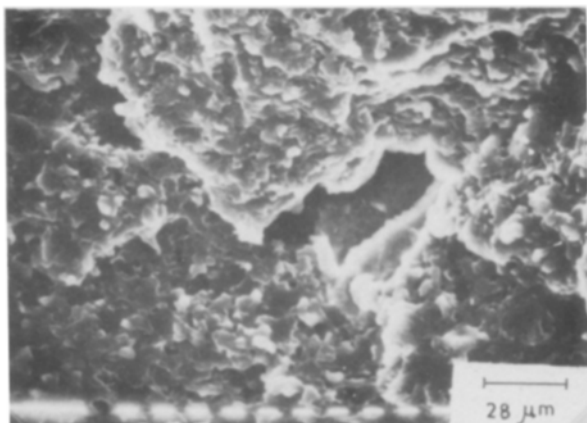


Figure 7 Tear failure surface of E<sub>30</sub><sup>d</sup> showing brittle-type failure.

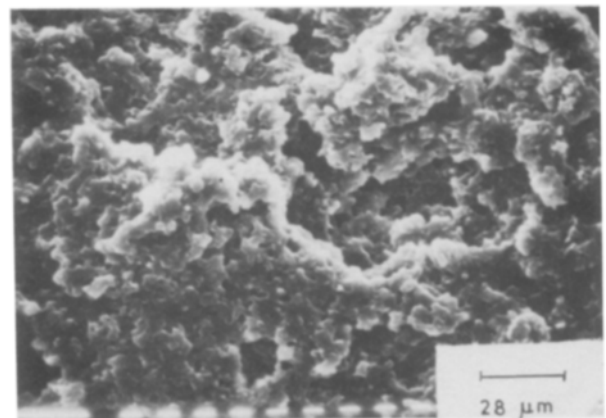


Figure 9 Tear failure surface of E<sub>50</sub><sup>d</sup> showing elastic-type deformation.

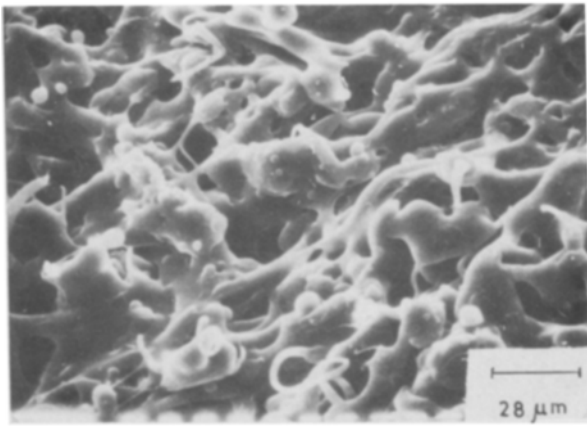


Figure 10 Tear failure surface of E<sub>70</sub> showing continuous dimples and fibrils.

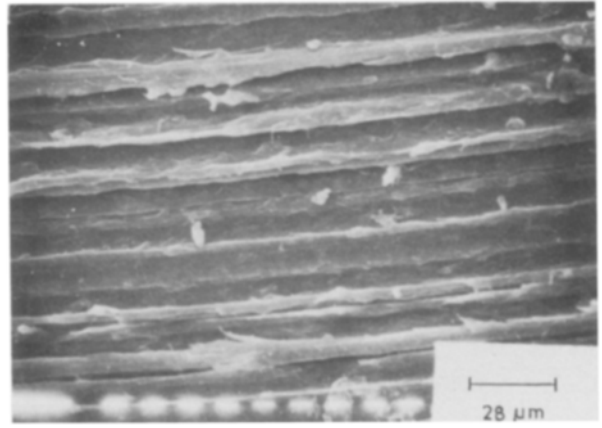


Figure 13 Abraded surfaces of PP showing many parallel grooves.

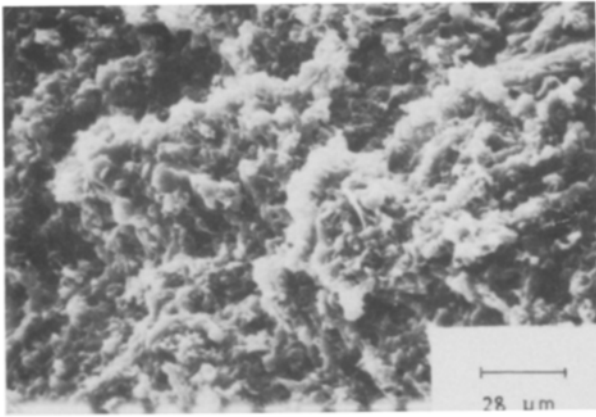


Figure 11 Tear failure surface of E<sub>70</sub><sup>d</sup> showing elastic-type deformation.

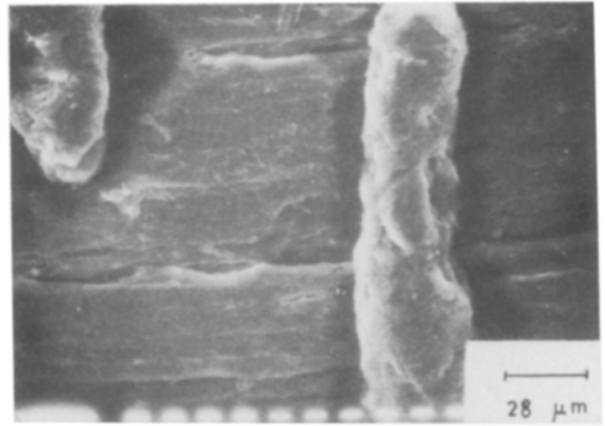


Figure 14 Abraded surface of E<sub>30</sub> showing grooves and abraded particles.

observed decrease in abrasion resistance (increase of volume loss) of the blends with an increase of rubber content is associated with the decrease in mechanical strength of the system. In the case of the uncrosslinked blends, the higher volume loss at higher proportions of EVA is due to the continuous nature of the rubber

phase. The decrease in abrasion resistance of the dynamically crosslinked high plastic blends ( $\geq 50\%$ ) as compared to the uncrosslinked blends is due to the degradation of PP phase which reduces the matrix strength (Table III), causing an increase in the rate of wear. But when the rubber content is higher and forms

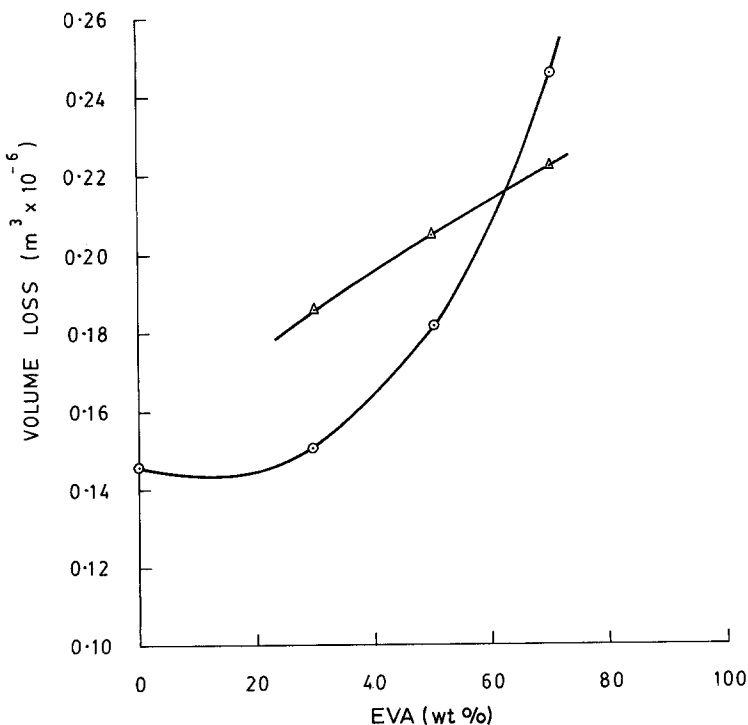


Figure 12 Effect of weight percentage of EVA on volume loss during wear: (○) uncrosslinked, (Δ) dynamically crosslinked.

TABLE III Mechanical properties of the blends

Mix No.	Mechanical property			
	Tensile strength (MPa)	Modulus at 50% elongation (MPa)	Hardness (Shore D)	Flexural modulus (MPa)
E <sub>0</sub>	41.79	–	74	1157
E <sub>30</sub>	21.04	20.40	62	435
E <sub>30</sub> <sup>d</sup>	18.03	18.03	59	332
E <sub>50</sub>	13.80	13.80	45	185
E <sub>50</sub> <sup>d</sup>	9.73	8.89	44	131
E <sub>70</sub>	3.17	2.75	14	9.52
E <sub>70</sub> <sup>d</sup>	5.39	4.00	27	52.4
E <sub>100</sub>	3.60	0.18	6	–

a continuous phase, dynamic crosslinking imparts high strength to the rubber phase. This increases the wear resistance.

### 3.2.1. Wear fractographs

Scanning electron microscopic observations of the abraded surfaces of the blends show that there is a change in the mode of abrasion as the rubber content increases ( $\geq 50\%$ ). The abraded surface of PP (Fig. 13) shows deep parallel grooves parallel to the direction of abrasion, which are characteristic of abrasive-type wear for thermoplastic materials. The abraded surface of E<sub>30</sub> (Fig. 14) shows less intense grooves compared to those of PP. The separation of particles is also visible on the surface. The dynamically crosslinked sample E<sub>30</sub><sup>d</sup> also shows a similar fracture topography with little variation (Fig. 15). In this case the grooves are more in number and are intense. Particle removal appears to be faster here. As the proportion of the rubber increases to 50%, the fracture topography completely changes. This is evident from the failure surface of E<sub>50</sub> (Fig. 16), which shows vertical ridges in a direction perpendicular to the direction of abrasion. This is a characteristic of frictional-type wear [16, 19]. The corresponding dynamically crosslinked sample (E<sub>50</sub><sup>d</sup>) shows cracks and deformed particles (Fig. 17). Unlike E<sub>50</sub>, in this case the ridge formation is not prominent. The formation of cracks may be due to the poor matrix strength of E<sub>50</sub><sup>d</sup> as compared to E<sub>50</sub> (Table III) due to degradation of the PP phase. As the rubber content further increases to 70%, the abraded surface shows highly deformed ridges (Fig. 18). This is due to the fact that in this case, since the rubber forms a

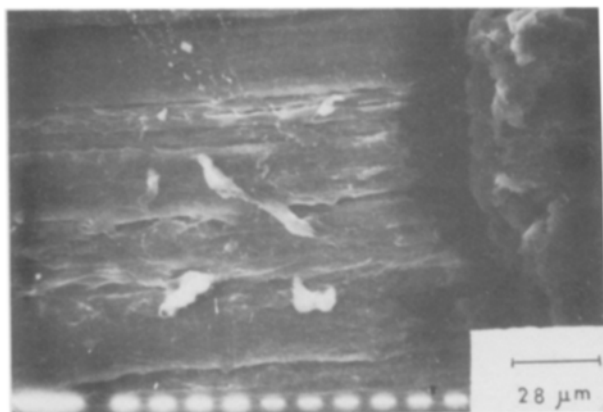


Figure 15 Abraded surface of E<sub>30</sub><sup>d</sup> showing parallel grooves and separation of particles.

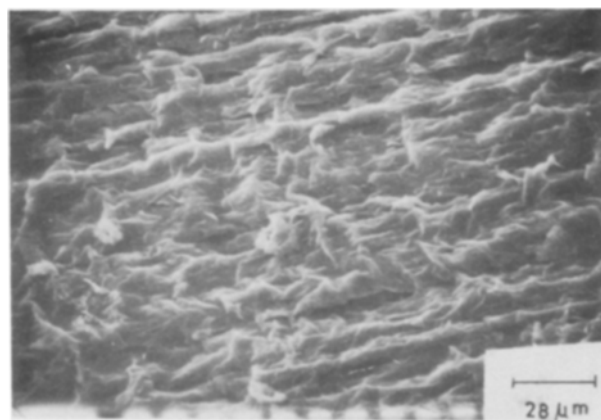


Figure 16 Abraded surface of E<sub>50</sub> showing closely spaced ridges.

continuous phase, the matrix strength is considerably reduced. As a result of this, the system cannot withstand the abrasive forces. The dynamically crosslinked blend (E<sub>70</sub><sup>d</sup>) shows more stable ridges as compared to E<sub>70</sub> (Fig. 19). This is because crosslinking of the continuous rubber phase increases the matrix strength (Table III) so that it can resist the abrasive forces. Nevertheless, the ridges are widely spaced and less prominent than in E<sub>50</sub>, indicating lower wear resistance than E<sub>50</sub>.

## 4. Conclusions

The present study indicates that the tear and wear resistance of thermoplastic elastomers from blends of ethylene vinyl acetate rubber and poly(propylene) increase with increasing proportion of the plastic phase. When the rubber phase is more ( $> 60\%$ ) and continuous in nature, the dynamic crosslinking increases the wear and tear properties as compared to those of the uncrosslinked blends. At lower proportions of the rubber phase, dynamic crosslinking hampers both the properties due to degradation of the PP phase. For both the uncrosslinked and crosslinked systems, the wear properties were dependent on the mechanical strength. Improved wear properties were obtained with increasing mechanical strength. Scanning electron microscopic examination of the tear failure surface of PP showed brittle-type failure. In the case of the uncrosslinked blends, as the proportion of the rubber phase increases the failure topography changes from brittle to ductile. The dynamically crosslinked samples containing higher proportions of



Figure 17 Abraded surface of E<sub>50</sub><sup>d</sup> showing cracks and deformed matrix.

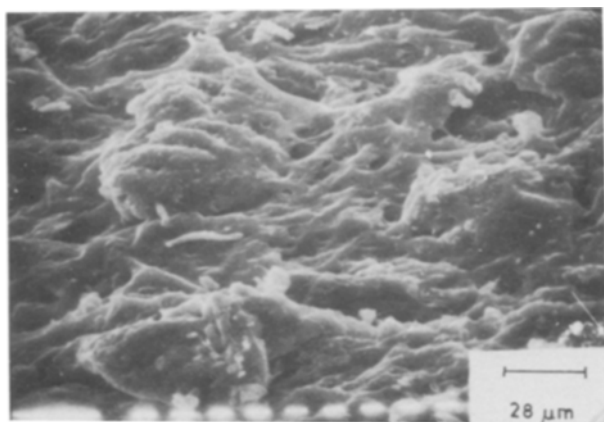


Figure 18 Abraded surface of E<sub>70</sub> showing deformed ridges.

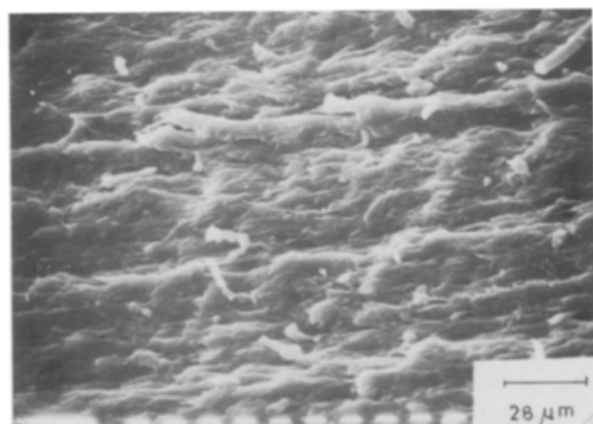


Figure 19 Abraded surface of E<sub>70</sub><sup>d</sup> showing widely spaced ridges.

rubber phase showed elastic-type failure. The SEM studies on the abraded surfaces show that there is a change in the mechanism of abrasion of the blends with an increase in the proportion of the elastomer phase, and that this change from abrasive-type wear to frictional-type wear occurs at higher proportions ( $\geq 50\%$ ) of the rubber phase.

## References

1. B. M. WALKER, "Handbook of Thermoplastic Elastomers" (Van Nostrand Reinhold, New York, 1979).
2. L. MULLINS, *Rubb. Devel.* **31** (1978) 92.
3. J. C. WEST and S. L. COOPER, "Science and Technology of Rubber", edited by F. R. Eirich (Academic, New York, 1978) Ch. 13.
4. A. WHELAN and K. S. LEE, "Development In Rubber Technology-3, Thermoplastic Rubbers", (Applied Science, London, 1982).
5. W. K. FISHER, US Patent 3 835 201 (1972).
6. D. J. ELLIOTT, *Natural Rubber Technol.* **12** (1981) 59.
7. D. S. CAMPBELL, D. J. ELLIOTT and M. A. WHEELANS, *ibid.* **9** (1978) 21.
8. W. K. FISHER, US Patent 3 758 643 (1971).
9. A. Y. CORAN and R. P. PATEL, *Rubb. Chem. Technol.* **53** (1980) 141.
10. *Idem, ibid.* **54** (1981) 91.
11. *Idem, ibid.* **54** (1981) 892.
12. B. KURIAKOSE and S. K. DE, *Polym. Engng Sci.* **25** (1985) 630.
13. A. SCHALLAMACH, *Proc. Phys. Soc.* **B67** (1954) 883.
14. *Idem, Trans. Inst. Rubb. Ind.* **28** (1952) 256.
15. G. S. KLITENIK and S. B. RATNER, in "Abrasion of Rubbers", edited by D. I. James (Maclaren & Sons, London, 1967) p. 64.
16. M. M. REZNIKOVSKII and G. I. BRODSKII, in "Abrasion of Rubber" edited by D. I. James (Maclaren & Sons, London, 1967) p. 14.
17. J. K. LANCASTER, in "Polymer Science", edited by A. D. Jenkins, (North-Holland, Amsterdam, 1972) Ch. 14, p. 960.
18. S. THOMAS, B. KURIAKOSE, B. R. GUPTA and S. K. DE, *J. Mater. Sci.* **21** (1986) 711.
19. S. THOMAS, *Wear* **116** (1987) 201.
20. J. GLUCKLICK and R. F. LANDEL, *J. Appl. Polym. Sci.* **20** (1976) 121.
21. A. KADIR and A. G. THOMAS, *Rubb. Chem. Technol.* **54** (1981) 15.
22. G. B. BUCKNALL and R. R. SMITH, *Polymer* **6** (1965) 437.
23. J. A. SCHMITT and H. KESKKULA, *J. Appl. Polym. Sci.* **3** (1960) 132.
24. W. D. BASCOM, R. E. COTTINGHAM, R. L. JONES and P. PEYSER, *ibid.* **19** (1975) 2545.
25. S. KUNZ-DOUGLASS, P. W. R. BEAUMONT and M. F. ASHBY, *J. Mater. Sci.* **15** (1980) 1109.
26. W. D. BASCOM, *Rubb. Chem. Technol.* **50** (1977) 327.
27. A. K. BHOWMICK, S. BASU and S. K. DE, *ibid.* **53** (1980) 321.
28. N. M. MATHEW and S. K. DE, *Polymer* **23** (1982) 632.
29. B. KURIAKOSE and S. K. DE, *J. Mater. Sci.* **20** (1985) 1864.
30. *Idem, J. Mater. Sci. Lett.* **4** (1985) 455.
31. S. THOMAS, B. R. GUPTA, S. K. DE and K. T. THOMAS, *Radiat. Phys. Chem.* **28** (1986) 283.
32. S. THOMAS, B. R. GUPTA and S. K. DE, *J. Vinyl Technol.* in press.
33. S. THOMAS, *Int. J. Polym. Mater.* in press.
34. S. THOMAS, B. KURIAKOSE, B. R. GUPTA and S. K. DE, *Plast. Rubb. Process. Appl.* **6** (1986) 101.
35. S. THOMAS, B. R. GUPTA and S. K. DE, *Kaut. Gummi. Kunstst.* in press.
36. E. MARTUSCELLI, C. SILVESTRE and G. ABATE, *Polymer* **23** (1982) 229.
37. Z. BARTCZAK, A. GALESKI and E. MARTUSCELLI, *Polym. Engng Sci.* **24** (1984) 1155.
38. L. ENGEL, H. KLINGELE, G. W. EHRENSTEIN and H. SCHAFER, "An Atlas of Polymer Damage", translated by M. S. Welling (Wolfe, London, 1981) p. 152.
39. S. W. ZHANG, *Rubb. Chem. Technol.* **57** (1984) 755.
40. G. S. KLITENIK and S. B. RATNER, *Soviet Rubb. Technol.* **19** (1960) No. 3.

Received 8 October 1986  
and accepted 19 January 1987